Naval Research Laboratory
Washington, DC 20375-5320

NRL/MR/6110--04-8775

Report on Radiocarbon Analysis of Surface Sediments from the Fore-Arc Basin of Nankai Trough

JOHN W. POHLMAN
REBECCA E. PLUMMER
CLARK S. MITCHELL

Geo-Centers, Inc.
Lanham, MD

KENNETH S. GRABOWSKI
DAVID L. KNIES
RICHARD B. COFFIN

Chemical Dynamics and Diagnostics Branch
Chemistry Divison

June 7, 2004

REPORT DOCUMENTATION PAGE

Form Approved
OMB No. 0704-0188

1. REPORT DATE *(DD-MM-YYYY)*	2. REPORT TYPE	3. DATES COVERED *(From - To)*
7 June 2004	Memorandum report	

4. TITLE AND SUBTITLE

Report on Radiocarbon Analysis of Surface Sediments from the Fore-Arc Basin of Nankai Trough

5a. CONTRACT NUMBER

5b. GRANT NUMBER

5c. PROGRAM ELEMENT NUMBER

6. AUTHOR(S)

John W. Pohlman,* Kenneth S. Grabowski, David L. Knies, Rebecca E. Plummer,* Clark S. Mitchell,* and Richard B. Coffin

5d. PROJECT NUMBER

5e. TASK NUMBER

5f. WORK UNIT NUMBER

7. PERFORMING ORGANIZATION NAME(S) AND ADDRESS(ES)

Naval Research Laboratory, Code 6114
4555 Overlook Avenue, SW
Washington, DC 20375-5320

8. PERFORMING ORGANIZATION REPORT NUMBER

NRL/MR/6110--04-8775

9. SPONSORING / MONITORING AGENCY NAME(S) AND ADDRESS(ES)

AIST C-7
Tsukaba
305-8567 Japan

10. SPONSOR / MONITOR'S ACRONYM(S)

11. SPONSOR / MONITOR'S REPORT NUMBER(S)

12. DISTRIBUTION / AVAILABILITY STATEMENT

Approved for public release; distribution is unlimited.

13. SUPPLEMENTARY NOTES

*Geo-Centers, Inc., Lanham, MD

14. ABSTRACT

Understanding the fate of methane carbon in anaerobic marine sediments is a critical component of evaluating the resource potential of hydrates and gas deposits in the ocean. Radiocarbon analysis of the total organic carbon (TOC) and total inorganic carbon (TIC) on 30 sediment samples from two mutlicores and six piston cores was performed to investigate the fate of methane carbon in sediment of the Nankai Trough. The TIC pool had consistently lower $\Delta^{14}C$ values compared to the TOC pool. A small deficit was expected from source reservoir differences during the biogenic production of TOC and TIC during and after sediment deposition. However, a large difference was observed in some samples, probably generated by a fossil carbon source after sediment deposition. We suggest this source of fossil carbon is from anaerobically oxidized fossile methane. Using a ^{14}C based isotope-mixing model, we calculated the potential contribution of methane carbon to the TIC pool. Model inputs to TIC were a near radiocarbon dead methane end member ($\Delta^{14}C_{AOM}$) from anaerobic oxidation of methane (AOM) and the $\Delta^{14}C_{TOC}$, which was normalized for reservoir effects and served as a proxy for the biogenic inorganic carbon (BIC) end member $\Delta^{14}C_{BIC}$. Two cores, presumed to represent control sites, indicate insignificant contributions from the methane end member. The TIC in one core appears to be almost entirely derived from AOM, and three cores show moderate levels of methane carbon input, with a preference towards higher fractions of methane in the TIC pool downcore. The patterns we observed in the data provide clear evidence that a combination of biogeochemical factors can influence $\Delta^{14}C$ of the TIC and TOC pools in the sediment. Furthermore, the data suggests that the TIC pool in the sediment can incorporate a large amount of C from fossil methane sources. However, the conclusions drawn from the dataset are preliminary and require basic geochemical, geophysical, and geological data from the cores and study site to ensure their validity.

15. SUBJECT TERMS

Hydrates; Radiocarbon; Nankai Trough

16. SECURITY CLASSIFICATION OF:			17. LIMITATION OF ABSTRACT	18. NUMBER OF PAGES	19a. NAME OF RESPONSIBLE PERSON
a. REPORT	b. ABSTRACT	c. THIS PAGE			Richard B. Coffin
Unclassified	Unclassified	Unclassified	UL	24	19b. TELEPHONE NUMBER *(include area code)* (202) 767-0065

Standard Form 298 (Rev. 8-98)
Prescribed by ANSI Std. Z39.18

CONTENTS

REPORT ON RADIOCARBON ANALYSIS OF SURFACE SEDIMENTS FROM THE FORE-ARC BASIN OF NANKAI TROUGH

BACKGROUND

Over the last decade large deposits of methane hydrate have been identified along continental margins. This observation presents a complex issue with strong international financial, environmental and scientific interests at stake. Several nations (in particular, Japan and India) have initiated studies assessing methane hydrates as a potential energy resource. The results of these studies may impact the global economy. Key uncertainties for energy extraction are the density, spatial variation, stability and fate of methane hydrates. It is imperative that each of these uncertainties is addressed. The data in this report is intended to offer insight into the fate of methane in anaerobic marine sediments of the Nankai Trough.

Methane hydrates are also relevant to basic earth science questions. For example, the world ocean carbon models currently focus on the dynamics of phytoplankton production. Hydrates and other benthic energy sources, including mud volcanoes, cold seeps, thermal vents, and brine pools are now becoming recognized as an abundant source of energy that support biota in and on the ocean floor. This biogeochemical activity needs to be integrated into the ocean carbon model, and should be considered when evaluating the environmental impact of mining methane hydrate formations.

Furthermore, there are important safety and environmental issues related to hydrate stability. Because methane is potent greenhouse gas (20x more effective than CO_2), a large release from seafloor hydrates could impact the global climate. A small (~1°C) increase in bottom-water temperature could disrupt the depth and thickness of the hydrate stability zone, which could release large quantities of methane from the seafloor and damage seafloor mounted platforms and equipment.

Consequently, it is important to understand the source, fate, and stability of the methane fluxes that contributes to formation of natural methane hydrate reservoirs.

INTRODUCTION AND APPROACH

In evaluating the resource potential of hydrate and gas deposits in the ocean, it is important to understand the natural fate of the methane carbon in the sediments (Fig 1- simple conceptual model). The objective of this study was to analyze radiocarbon isotopes of sediment organic and inorganic carbon to identify the fate of methane carbon into these pools. In particular, we will evaluate the discrepancy of the $\Delta^{14}C$ between the total organic carbon (TOC) and total inorganic carbon (TIC)[1] in the sediment carbon pool to determine what fraction of the TIC pool is derived from the anaerobic oxidation of methane (AOM) (Eq. 1). AOM is the most significant sink for methane in anaerobic marine sediments and could account for the removal of up to 90% of the methane generated within marine sediments (Reeburgh, 1996).

$$CH_4 + SO_4^{-2} \rightarrow HCO_3^- + HS^- \qquad \text{(Eq.1)}$$

[1] In the context of this report TIC refers to the solid carbonate fraction in the sediments and excludes the dissolved inorganic carbon (DIC) in the pore water.

Manuscript approved March 12, 2004.

A ^{14}C-based isotope-mass-balance model was implemented to make this calculation. Due to the lack of geological and geochemical information on the samples we received, the conclusions drawn in this report were based on a number of assumptions. The assumptions are explicitly stated and are subject to modification as we receive basic information about these cores.

Application of a two-source isotope-based mixing model (Eq. 2), requires that the isotopic ratio of the endmembers are well constrained. In this case, we are evaluating the contribution of methane carbon into the TIC ($\Delta^{14}C_{TIC}$), from a mixture of biogenic inorganic carbon (BIC, $\Delta^{14}C_{BIC}$) and AOM derived carbon ($\Delta^{14}C_{AOM}$). In the equation, "f" is the fractional contribution of the methane endmember. The BIC endmember is assumed to originate from calcareous material deposited on the seafloor that has been buried, buried dissolved inorganic carbon (DIC) and respired DIC, while the AOM endmember is a product of precipitation of AOM derived DIC in the sediments. Since we do not physically separate the carbonaceous material in the sediments, we are not concerned that biogenic DIC (buried and respired) and methane derived DIC co-precipitate as carbonate in sediments.

$$\Delta^{14}C_{TIC} = (f_{AOM})\,\Delta^{14}C_{AOM} + (1-f_{AOM})\,\Delta^{14}C_{BIC} \qquad \text{(Eq. 2)}$$

The $\Delta^{14}C$ of the CH_4 endmember is be assumed to be –992±6‰. This is the average $\Delta^{14}C$ from 21 hydrate samples collected from a mixture of bacterial and thermogenic hydrate methane samples at Blake Ridge, the Gulf of Mexico, the Northern Cascadia Margin and the Haakon Mosby mud volcano. These data were recently analyzed at NRL and described by Pohlman et al. (2003). This assumed radiocarbon value is severely ^{14}C-depleted and indicates that both bacterial and thermogenic methane associated with methane hydrates are near radiocarbon dead (^{14}C-depleted). A similar observation of radiocarbon dead bacterial methane has recently been reported from the Northern Gulf of Mexico (Sassen et al., 2003). We speculate that our observations are representative of all marine sediments and welcome the opportunity to analyze methane samples from the Nankai Trough.

The uniformly low $\Delta^{14}C$ of methane makes it an excellent tracer for determining the contribution of methane into different carbon pools. Not only is the source $\Delta^{14}C$ of the methane well constrained, the absence of ^{14}C in methane precludes fractionation during methane assimilation. Stable carbon isotope signatures of methane found in gas hydrate bearing sediments have a wide range of values between –40‰ to –120‰. The reason for this variation is a function of the source (e.g., biogenic or thermogenic) and diagenetic alterations the methane has undergone. This broad range of values and fractionation that occurs during methane cycling complicates application of stable isotope mixing models using the $\delta^{13}C$ signature of CH_4 as an endmember.

Application of radiocarbon as a tracer is confounded by the radioactive decay of ^{14}C. Determining whether or not the measured $\Delta^{14}C$ values are a product of radioactive decay or dilution by radiocarbon dead CH_4 must be resolved.

In the model, the $\Delta^{14}C$ of the biogenic inorganic carbon (BIC) endmember is represented by the $\Delta^{14}C$ of the total organic carbon (TOC), corrected for reservoir effects. This assumption hinges on the assumption that the TOC is not significantly altered by AOM and, therefore, is a suitable proxy for BIC (also not altered by AOM). Using the TOC as a proxy for $\Delta^{14}C_{BIC}$ is based on the following assumptions:

1. Cores B003-PC01 and B003-PC02 are unaffected by AOM and will be used as control cores. If there was no significant flux of methane at these sites ($f_{AOM} = 0$: Eq 2.), $\Delta^{14}C_{TIC}$ is equivalent to $\Delta^{14}C_{BIC}$. We were given no information on the gas flux from these sites and are basing this assumption on the interpretation of our data and our recollection of conversations during previous correspondence.

2. The $\Delta^{14}C_{TIC}$ and $\Delta^{14}C_{TOC}$ from cores B003-PC01 and B003-PC02 are representative of $\Delta^{14}C_{BIC}$ and $\Delta^{14}C_{TOC}$ for the entire study region.

3. The intra-core variation of the $\Delta^{14}C$ of the TOC in all cores is entirely a function of radioactive decay since deposition. However, AOM is mediated by microbes that acquire their carbon from methane and the microbes are a component of the TOC pool (Fig. 1). Thus, the production of DIC by AOM (which precipitates as TIC) is accompanied by production of TOC. However, since the free energy yield of AOM is very low, large quantities of methane must be oxidized to form small quantities of biomass (a component of the TOC pool). Consequently, the alterations to the TIC pool should be significantly greater than those in the TOC pool. The flaw in this assumption will lead to a small underestimation in the fractional contribution by methane.

4. The offset between the $\Delta^{14}C_{TIC}$ and $\Delta^{14}C_{TOC}$ of cores B003-PC01 and B003-PC02 resulted from reservoir effects associated with the source of the TOC and TIC. For example, the buried TIC may be a product of biological assimilation from deeper "older" DIC and near-surface "younger" DIC, while the TOC may be a product of biological assimilation of near-surface "younger" DIC and, possibly, terrestrial organic matter. In order to utilize the $\Delta^{14}C_{TOC}$ as a proxy for the $\Delta^{14}C_{BIC}$, an offset factor α was applied to the $\Delta^{14}C_{TOC}$ to normalize it to $\Delta^{14}C_{BIC}$ (Eq. 3). The offset factor α was calculated based on the average $\Delta^{14}C_{TOC}$ and $\Delta^{14}C_{TIC}$ from all samples in control cores PC-01 and PC-02 (Eq. 4).

$$\Delta^{14}C_{BIC} + 1000 = \alpha * (\Delta^{14}C_{TOC} + 1000) \qquad \text{(Eq. 3)}$$

$$\alpha = (\text{Average } (\Delta^{14}C_{TIC}) + 1000)/ (\text{Average } (\Delta^{14}C_{TOC}) + 1000) \qquad \text{(Eq. 4)}$$

5. The reservoir effects observed in the control cores PC-01 and PC-02 are the same for every core. By this assumption, it is valid to utilize α to normalize every $\Delta^{14}C_{TOC}$ value to the $\Delta^{14}C_{BIC}$ endmember in the mixing model (Eq. 2).

METHODS

Sample Selection

Sediment samples were taken from cores collected during the Bosei-maru cruise in the Nankai Trough during 26 November–6 December 2003. A total of 37 sediment samples were selected for possible radiocarbon analysis by accelerator mass spectrometry (AMS) at the Naval Research Laboratory (NRL). These 37 samples were collected from various depths from 11 different cores. All 37 were packaged in dry ice, and shipped to NRL. Unfortunately, due to delays in shipping, the samples thawed and warmed to 12–15°C upon delivery to NRL. They were quickly placed in a freezer held at –20°C until subsequent processing. From the original 37 samples delivered to NRL, Prof. Matsumo and Dr. Tanahashi selected 30 for AMS analysis. Table I lists the 30 samples chosen and information we have about their core location.

Sample Preparation and Purification

Sediment Carbonates (Total Inorganic Carbon (TIC). Sediment samples were removed from the freezer, transferred into 20 ml scintillation vials and freeze-dried overnight. Freeze dried samples were homogenized with a mortar and pestle and transferred to clean vials. Based on the measured percentage of inorganic carbon in the sediments, a mass of sediment that would produce 1-3 mg of C as CO_2 upon carbonate digestion (depending upon quantity of sample available) was transferred into a quartz carbonate digester. Two ml of 85% H_3PO_4 saturated with $CuSO_4$ was added to the side arm of the digester, and a small stir bar was placed in the bottom of the reactor tube. The digester was placed on a vacuum manifold and evacuated for 10 minutes, or until the pressure was reduced to 1-2 Torr. The evacuated reactor was removed from the vacuum manifold and the $H_3PO_4/CuSO_4$ mixture was poured from the side arm onto the sample. The sample was placed on a stir plate for 2 hours to allow the carbonate to dissolve in the acid solution. The $CuSO_4$ was added to precipitate any volatile sulfides produced during the carbonate acidification. Addition of the stir bar ensured complete carbonate dissolution and exposure of the volatile sulfides to precipitation by the $CuSO_4$.

The digester was placed on the NRL cryogenic distillation/graphitization apparatus (Pohlman et al., 2000). Carbon dioxide was cryogenically separated from the gas mixture in the digester by a series of low-pressure cryogenic distillations using a dry ice/ethanol slurry and liquid nitrogen. The purified sample was transferred to a molar quantification unit where the mass of carbon recovered from the sample was determined manometrically. The entire sample was transferred to a volume manipulator unit where 1 mg of the sample was split using a gas-tight syringe, which operates like a bellows. The 1 mg C gas sample was transferred to the graphitization reactor. Procedures for converting the carbon dioxide sample to graphite are described below.

Total Organic Carbon (TOC). A quantity (about 2-ml) of the freeze-dried and homogenized sediment samples was placed in a 50-ml pyrex centrifuge tube. Then 35-40 ml of 10% HCl were added to the centrifuge tubes to hydrolyze the carbonates. The

samples were stirred with a stainless steel stirring rod and were then placed on a heating block (60-90°C) for 6 hours. The samples were stirred every hour during the carbonate digestion to ensure the entire sample was constantly exposed to acidic conditions. After the acid hydrolysis, the samples were centrifuged at 1000 rpm for 5 minutes. The acid solution was decanted and replaced by deionized (DI) water. The sample was homogenized by stirring and centrifuged to rinse the acid from the sample. This process was repeated 4 times or until the pH of the supernatant was equivalent to fresh DI water (pH=4-5).

The samples were placed back in the freeze-dryer and left overnight. A quantity of the sample (100-300 mg) that would produce 1-3 mg carbon (based on EA analysis of select samples) upon combustion was transferred into a smallVycor tube. Then, 200 mg of copper oxide and several grains of silver were added into the tube. Copper oxide provides oxygen during sample combustion while the silver grains serve as a sulfur trap. The small Vycor tube was placed inside a 3/8" Vycor tube to prevent silica in the sample from reacting with and cracking the exterior tube. The 3/8" Vycor tubes were placed on a vacuum manifold and evacuated for 6-12 hours or until the pressure was nominally 50 mTorr. The tubes were flame sealed under vacuum and transferred to a muffle furnace, combusted at 900° C for 6 hours and then slow cooled.

Combusted samples were inserted into a break-seal and introduced to the NRL cryogenic distillation/graphitization apparatus. Carbon dioxide was cryogenically separated from the gas mixture present in the digester by a series of low-pressure cryogenic distillations using a dry ice/ethanol slurry and liquid nitrogen. The purified sample was transferred to a molar quantification unit where the mass of carbon recovered from the sample was determined manometrically. The entire sample was transferred to a volume manipulator unit where 1 mg of the sample was split using a gas-tight syringe that operates like a bellows. The 1 mg C gas sample was transferred to the graphitization unit. Procedures for converting the carbon dioxide sample to graphite are described below.

Graphitization

Prior to transferring the samples into the graphitization reactors, 1 mg of elemental Fe was placed in a culture tube inside each reactor. The reactor was then loaded with 1 atm of H_2 and heated to 450°C for 2 hrs. This process purified the Fe and activated it as a catalyst for reducing CO_2 to graphite. The reactors were then evacuated in order to introduce the samples.

Once all reactors were loaded with CO_2, the reactor manifold was filled with 1 atm of cryogenically purified H_2. The CO_2 in each reactor was frozen with liquid nitrogen and then H_2 was added to each reactor from the manifold. The ratio of H_2 to CO_2 was 2.5, which is in excess of the reaction stoichiometry of 2:1. The Fe was then heated to 600°C for 6 hours, well beyond the time required for complete reduction of CO_2 to graphite. Pressure and temperature profiles for each reactor were logged by a LabVIEW application developed for this system. A cold finger at the bottom of the

reactor removed water produced during the reduction of CO_2 that could interfere with the graphitization process. The resulting graphite was delivered to the NRL TEAMS-AMS facility where it was pressed into a 1-mm-diameter hole in an aluminum target holder used as a "cathode" for the AMS measurement.

Reactor Contamination. We encountered problems with graphitizing a number of the TOC samples. On the first attempt, 15 of the 30 samples failed to produce graphite. The most likely suspect for the contamination was sulfur dioxide, which co-distills into the graphitization reactor with carbon dioxide. It is suspected that the SO_2 reduces to elemental sulfur on the surface Fe catalyst, thus preventing the catalyzed reduction of carbon dioxide to graphite. The occurrence of this problem is infrequent and not well understood. The prevalence of the problem in this set of samples was very unusual.

We recognized two solutions to this problem. First, since the addition of silver to the combustion tube normally alleviates sulfur poisoning, we altered the oven temperature cycle to increase the time for scrubbing sulfur from the sample. For 6 of the 15 failed samples this modification produced graphite in the normal manner. For the remaining 9 samples a second approach was employed. Carbon dioxide from the failed reactor was frozen out of the reactor for ten minutes using liquid nitrogen. The hydrogen was then pumped out of the failed sample, and the CO_2 was transferred to a reactor with fresh Fe catalyst. The reaction was repeated in the new reactor using the procedure described previously. Each of the samples produced graphite in the second reactor. These samples are denoted with an asterisk (*) in the data tables, and are referred to as "transfer" samples in this report.

To evaluate potential fractionation associated with the transfer process, the 6 samples processed by both the transfer technique and standard protocol were compared. The results were slightly and systematically different. Data from these six samples (see Table II) was used to create an algorithm to convert the value obtained from the transfer graphite into the value we would expect for graphite produced normally. The algorithms used for the TOC data were:

$$pM(normal) = K\ pM(transfer), \qquad \text{(Eq. 5)}$$

$$\Delta^{14}C(normal) = K\ (\Delta^{14}C(transfer) + 1000) - 1000, \text{ and} \qquad \text{(Eq. 6)}$$

$$CRA(normal) = CRA(transfer) - 8033\ \ln K \qquad \text{(Eq. 7)}$$

where pM is percent modern carbon, CRA is conventional radiocarbon age, and

$$K = 0.9221 \pm 0.0524$$

The coefficient K is derived from a least squares fit to the data available from the six paired samples. This algorithm was used to correct the ^{14}C data for the nine samples for which graphite was only produced using the transfer method. For the six samples that produced graphite by both methods, only values from the graphite produced normally

were used in the data analysis plots. The algorithm introduced a significant error to the converted data that was propagated through all subsequent calculations of the data.

Standards and Blanks

Standards and blanks were provided with each set of samples produced. The standard material used was the NIST Oxalic Acid II standard that was processed by combustion. The blank material used for the TOC analysis was a known radiocarbon-dead source of coal provided to NRL by the United States Geological Survey (USGS). The blank material used for the TIC analysis was the doublespar optical calcite used in the Third International Radiocarbon Intercomparison effort. The standards and blanks were treated exactly as the corresponding samples to reduce the effect of any contamination or fractionation that could occur during the sample pretreatment and graphite production procedures. There was no obvious evidence of sample contamination or fractionation for any of the standards or blanks.

General Laboratory Procedures

The glassware used in all laboratory procedures was cleaned by rinsing with DI water followed by baking in a muffle furnace at 450°C for 4 hours to remove all traces of carbon. Vycor tubes, copper oxide and silver were baked at 900°C prior to use. Nitrile gloves were worn during all sample handling procedures and all personnel in the lab were required to wear special protective clothing to minimize contamination of the lab and samples.

Accelerator Mass Spectrometry

Targets prepared in the NRL Graphite Lab were analyzed at the NRL AMS facility. This unique facility (Grabowski et al, 2000) is equipped with both a high intensity Cs sputter source used for ^{14}C analysis, and capabilities for a commercial secondary ion mass spectrometer (SIMS) used as an ion source for trace element analysis. Its low- and high-energy transport systems allow simultaneous transport and analysis of a broad mass range (Mmax/Mmin ~ 8). Features of the system for ^{14}C analysis include a forty sample multi-cathode ion source (model MC-SNICS) from National Electrostatics Corporation, a Pretzel recombinator magnet to simultaneously inject masses 12 to 14, a beam chopper to block mass 12 and 13 during measurement of ^{14}C, a 3 MV Pelletron tandem accelerator, an electrostatic 3° bend for charge state selection, a 30° electrostatic analyzer, and a split pole mass spectrograph for beam detection. Low noise Faraday cups and a solid-state detector measure the relevant beam intensities. The operator interface is based on the LabVIEW application, which monitors and controls all relevant system components via a fiber optic network. This system provides precise dating capabilities for ^{14}C analysis.

The data collection and analysis follows standard procedures described in a recent publication (Tumey et al, 2004). The sixty samples were measured amongst OX II standards and appropriate blanks distributed over four different loadings of the sample

wheel. On average, each wheel contained 2 AMS blanks for tuning the accelerator, 3 processing blanks appropriate for the samples on the wheel, and 7 OX II standards. We obtained $\delta^{13}C$ results from GC-IRMS analysis of the sediment samples. These values were used to calculate the $\delta^{13}C$ fractionation correction for each sample.

RESULTS AND DISCUSSION

Data for the TOC and TIC results are presented in Tables III and IV, respectively. The data are presented in three formats: $\Delta^{14}C$, percent modern carbon (*pM*) and conventional radiocarbon age (*CRA*) (see Eqns. 8–10). While the values of each expression are considerably different, they are all fundamentally based upon $^{14}C/^{12}C$ of the unknown R_s compared to $^{14}C/^{12}C$ of the NIST oxalic acid II standard R_{std}. The data are presented in these different formats to simplify different types of data interpretation.

$$\Delta^{14}C = \left[\frac{R_s}{R_{std}} - 1\right] \times 1000 \ (‰) \qquad \text{(Eq. 8)}$$

$$pM = \frac{R_s}{R_{std}} \times 100 \ (\%) \qquad \text{(Eq. 9)}$$

$$CRA = -8033 \ln\left[\frac{R_s}{R_{std}}\right] \text{(ybp)} \qquad \text{(Eq. 10)}$$

Each R is normalized to a fixed $\delta^{13}C$ based on the $\delta^{13}C$ for that sample (Table III and IV) to correct for isotope fractionation. R_{std} is corrected for decay of ^{14}C in the standard for $\Delta^{14}C$ and *pM*, but not for *CRA*, since *CRA* is taken relative to 1950 as the present (ybp stands for years before present). For a full description of reporting ^{14}C data see (Stuiver and Polach , 1977). Due to graphitization difficulties with transfer TOC samples, the measured results for those samples were adjusted as described in the methods section of this report, and reported as adjusted values in Table III.

The data from each core are represented graphically in Figure 2. Based on the limited information provided for these samples, we can make the following generalizations about the data.

1. Cores B003-MC01, B003-MC03, B003-PC01 and B003-PC02 are all relatively modern ($\Delta^{14}C$ for all samples is > –300‰). Aside from one outlier, the $\Delta^{14}C_{TOC}$ was consistently higher than the $\Delta^{14}C_{TIC}$. This difference, which is fairly consistent among all the samples in these four cores, is most likely due to reservoir effects that affected the age of these carbon pools when they were formed. Cores B003-PC01 and B003-PC02 are assumed to represent control cores where the flux of methane was minimal.

2. Core B003-PC03 had the lowest $\Delta^{14}C$ values among all the cores, with $\Delta^{14}C_{TIC}$ considerably lower than $\Delta^{14}C_{TOC}$. This core was unusual in that the downcore

profile showed no variation. This pattern suggests these sediments were deposited instantaneously as one homogeneous layer at some time in the past. The large discrepancy between the $\Delta^{14}C_{TIC}$ and $\Delta^{14}C_{TOC}$ suggests a process other than reservoir effects has altered one or both of the carbon pools. We suggest this alteration was due to production of radiocarbon dead DIC from anaerobic oxidation of radiocarbon dead methane that precipitated as carbonate.

3. Cores B003-PC05, B003-PC06 and B003-PC07 display consistently more negative $\Delta^{14}C$ values as you progress downcore, TIC values were all more negative than the TOC, and there was increasing downcore disparities between the $\Delta^{14}C_{TIC}$ and $\Delta^{14}C_{TOC}$. The increasing downcore disparity is the most distinctive feature of these cores and suggests the contribution of methane carbon to the TIC increases downcore. This pattern is consistent the fact that the zone of AOM is typically deeper in the core. Given the total core length information provided to us, this pattern suggests the sulfate methane interface (SMI) may be deeper than 423 cm (Table I, with core length info).

Sedimentation Rate

While we were not provided depth intervals for each core sample, we can estimate the maximum apparent sedimentation rates *S* for each core based on the overall core length and the difference in the CRA between the topmost and bottommost samples. Table V lists the outcome of this analysis using the TOC to represent the age of the sediment. The result is perplexing in that very high apparent sedimentation rates are obtained for most cores with sufficiently good statistics, except for PC05, which has $S \sim$ 10 cm/ka, and MC01 and PC03 which have an inverted behavior in the TOC. This analysis suggests there is some odd behavior effecting the apparent age of the sediment with depth in most cores.

Model Output

To apply the ^{14}C-based isotope-mixing model we needed to evaluate the offset factor α (see Eq. 3 and 4). As Figure 3 shows, the relevant ratio to compute α was quite uniform amongst all samples from cores PC01 and PC02. When averaged, we obtained

$$\alpha = 0.9295 \pm 0.0545$$

This offset factor takes into account the radioactive decay of ^{14}C, so that depth dependent behavior of biogeochemical processes can more easily be discerned. As Fig 3 shows, this is apparently the case with cores PC03, PC05, PC06 and PC07. Upon solving for f_{AOM} in Eq. 2 using α and the relationship shown in Eq 3, we obtained the results provided inTable VI and shown graphically in Figure 4. The control cores B003-PC01 and B003-PC02 show no evidence of input from methane carbon into the TIC pool. Meanwhile, the model suggests the TIC in Core PC-03 is almost entirely a product of DIC produced from AOM. Results from Core PC-05 suggest a moderate input, while Cores PC-06 and PC-07 each suggest substantial input that increases downcore closer to the presumed SMI.

Although the conclusions drawn in this report are tentative, they provide evidence that the fate of a large fraction of carbon from anaerobically oxidized methane in gas-charged (possibly hydrate bearing) sediments is in the carbonate pool (referred to as TIC in the report). Similar suggestions have been made based on the observation of ^{13}C depleted $\delta^{13}C$ values from authigenic carbonate nodules collected near gas hydrate formations. Elvert et al. (2000) reported values as low as -48‰ from carbonate samples collected near cold seeps on the Aleutian subduction zone. It is interesting and important to note that the stable carbon isotope analysis of the samples analyzed in this study did not show similar depletion. The lowest $\delta^{13}C$ value measured in the TIC samples was -5.20‰. Without additional geochemical data it is impossible to explain this troubling inconsistency. The integrity of the $\delta^{13}C_{TIC}$ measurements is being verified and may be reanalyzed. A potential biogeochemical explanation is ^{13}C enrichment of the inorganic carbon pool by rapid methanogenesis. Methanogens preferentially assimilate the lighter ^{12}C isotope and have been reported to substantially enrich the DIC pool with ^{13}C (Claypool et al., 1985). Additional data and discussion with other scientists who participated in the project is required to resolve this discrepancy.

SUMMARY

Radiocarbon analysis of total organic carbon (TOC) and total inorganic carbon (TIC) was performed on 30 sediment samples from two multi-cores and six piston cores. With the exception of one sample, the TIC pool had lower $\Delta^{14}C$ values than the TOC, which indicates reservoir effects during the biogenic production of the TOC and TIC, and possibly a contribution from a fossil carbon source. We suggest this source of fossil carbon may be from anaerobically oxidized fossil methane. Using a ^{14}C based isotope-mixing model, we calculated the potential contribution of methane carbon in the TIC pool. Model inputs were a near radiocarbon dead methane endmember ($\Delta^{14}C_{AOM}$) and the $\Delta^{14}C_{TOC}$, which was normalized for reservoir effects and served as a proxy for the $\Delta^{14}C_{BIC}$ endmember. Two cores, presumed to represent control sites, indicate insignificant contributions from the methane endmember. The TIC in one core appears to be almost entirely derived from anaerobic methane oxidation and three cores show moderate levels of methane carbon input, with a preference towards higher fractions of methane in the TIC pool downcore.

Other than the data provided in this report, our interpretation was based upon core location, total core length and depth profiles in 2 of the 8 cores. The data evaluation and interpretation are based upon a large number of assumptions that must be addressed using data we suspect was generated as part of the complete project. Our conclusions are tentative and subject to change. We strongly suggest that basic geochemical, geophysical and geological data be provided to NRL so that we can validate our model and verify the conclusions presented in this report. The patterns we observed in the data provide clear evidence that a combination of biogeochemical factors strongly influence the $\Delta^{14}C$ of the TIC and TOC pools in the sediment.

REFERENCES

Claypool,G.E., C.N.Threlkeld, P.N.Mankiewicz, M.A.Arthur, and T.F.Anderson 1985. Isotopic composition of interstitial fluids and origin of methane in slope sediment of the Middle America Trench, Deep-Sea Drilling Project Leg-84. Initial Reports of the Deep Sea Drilling Project 84: 683-691.

Elvert,M., E.Suess, J.Greinert, and M.J.Whiticar 2000. Archaea mediating anaerobic methane oxidation in deep-sea sediments at cold seeps of the eastern Aleutian subduction zone. Org.Geochem. 31: 1175-1187.

Grabowski,K.S., D.L.Knies, T.M.DeTurck, D.J.Treacy, J.W.Pohlman, R.B.Coffin, and G.K.Hubler 2000. A report on the Naval Research Laboratory AMS facility. Nucl. Instr. and Meth. B 172: 34-39.

Pohlman,J.W., D.L.Knies, K.S.Grabowski, T.M.DeTurck, D.J.Treacy, and R.B.Coffin 2000. Sample distillation/graphitization system for carbon pool analysis by accelerator mass spectrometry (AMS). Nucl.Instr.Meth.B 172: 428-433.

Pohlman,J.W., N.R.Chapman, G.D.Spence, M.Whiticar, D.L.Knies, R.B.Coffin 2003. Thermogenic and Biogenic Gas Hydrates on the Northern Cascadia Margin: A Molecular, Isotopic and Geochemical Comparison. EOS. Trans. AGU, 84(46). Fall Meet. Suppl. Abstract OS52D-06.Reeburgh,W.S. 1996. "Soft spots" in the global methane budget, p. 334-342. *In* [eds.], M.E.Lidstrom and F.R.Tabita Microbial growth on C1 compounds. Kluwer Academic Publishers.

Sassen,R., A.V.Milkov, E.Ozgul, H.H.Roberts, J.L.Hunt, M.A.Beeunas, J.P.Chanton, D.A.DeFreitas, and S.T.Sweet 2003. Gas venting and subsurface charge in the Green Canyon area, Gulf of Mexico continental slope: evidence of a deep bacterial methane source? Org.Geochem. 34: 1455-1464.

Stuiver M, Polach HA (1977) Reporting of c-14 data - discussion. Radiocarbon 19:355-363. http://www.radiocarbon.org/Pubs/Stuiver/index.html

Tumey S.J., K.S. Grabowski, D.L. Knies, and A.C. Mignerey 2004. Data collection, filtering and analysis at the Naval Research Laboratory trace element accelerator mass spectrometry facility. Nucl. Instr. and Meth. B (accepted)

Table I. Location of Cores Selected for AMS Analysis

Sample Identification Nankai, 11/26–12/6, 2003	Latitude (°-')	Longitude (°-')	water depth (m)	core length (cm)	sample depth (cm)
PC01 N0. 19 1-5 (12/3)	33-45.743	136-27.603	2057	197	
B003-PC1-1					5
B003-PC1-2					35
B003-PC1-3					65
B003-PC1-4					115
B003-PC1-5					165
PC02 NO,20 (12/3)	33-50.003	136-25.924	1805	140	
B003-PC02-1					
B003-PC02-2					
B003-PC02-3					
B003-PC02-4					
B003-PC03 4T NO. 1 (12/4)	34-10.033	137-59.046	855	79	
B003-PC03-1					17.5
B003-PC03-2					22.5
B003-PC03-3					38
B003-PC03-4					67.5
PC05 NO, 8 (12/4)	34-14.057	137-40.247	1186	67	
B003-PCO5-1					
B003-PCO5-2					
B003-PCO5-4					
B003-PCO5-5					
PC06 NO. 9 (12/5)	34-12.327	137-27.562	1270	423.5	
B003-PC06-1					
B003-PC06-2					
B003-PC06-3					
B003-PC06-4					
B003-PC06-5					
B003-PC06-6					
PC07 NO. 10 (12/5)	34-10.570	137-25.343	1208	89	
B003-PC07-1					
B003-PC07-2					
B003-PC07-4					
MC01 NO. 19 (12/3)	33-45.735	136-27.555	2056	40	
B003-MC01-1					
B003-MC01-2					
MC03 NO. 9 (12/5)	34-12.222	137-27.656	1257	36	
B003 -MC03-1					
B003 -MC03-2					

Table II. Comparison of AMS results for TOC using normal and transfer methods

Sample	NRL ID (AMS)	$\delta^{13}C$ (‰)	$\sigma(\delta^{13}C)$ (‰)	$\Delta^{14}C$ (‰)	$\sigma(\Delta^{14}C)$ (‰)	CRA (ybp)	σ(CRA) (ybp)	pM (%)	σ(pM) (%)
PC03-1*	660	-21.67	0.04	-587.92	5.96	7,069.44	115.42	41.21	0.60
PC03-3*	659	-21.40	0.03	-546.95	6.85	6,305.80	122.38	45.30	0.68
PC05-2*	688	-20.89	0.03	-149.09	11.70	1,245.59	109.76	85.09	1.17
PC05-3*	689	-21.42	0.01	-411.83	8.64	4,212.04	117.20	58.82	0.86
PC05-4*	661	-21.57	0.03	-567.75	4.67	6,686.12	88.01	43.23	0.47
PC06-5*	657	-21.62	0.03	-526.79	8.34	5,958.27	140.70	47.32	0.83
PC03-1	721	-21.67	0.04	-608.28	3.97	7,475.82	80.94	39.17	0.40
PC03-3	722	-21.40	0.03	-605.32	3.67	7,417.77	76.30	39.47	0.37
PC05-2	742	-20.89	0.03	-305.86	6.94	2,881.28	79.82	69.41	0.69
PC05-3	726	-21.42	0.01	-430.39	5.16	4,470.77	72.34	56.96	0.52
PC05-4	723	-21.57	0.03	-583.83	5.26	6,990.70	100.94	41.62	0.53
PC06-5	674	-21.62	0.03	-438.90	15.89	4,599.34	226.28	56.11	1.59

* transfer sample, with raw AMS results

Table III. AMS results for analysis of TOC from Nankai sediment cores

Sample	NRL ID (AMS)	$\delta^{13}C$ (‰)	$\sigma(\delta^{13}C)$ (‰)	$\Delta^{14}C$ (‰)	$\sigma(\Delta^{14}C)$ (‰)	CRA (ybp)	σ(CRA) (ybp)	pM (%)	σ(pM) (%)
MC01-1	677	-21.22	0.01	-218.1	14.9	1925	152	78.2	1.5
MC01-2	727	-20.73	0.05	-42.0	8.2	293	69	95.8	0.8
MC03-1	678	-21.05	0.02	-93.6	7.6	737	68	90.6	0.8
MC03-2	679	-21.41	0.08	-158.9	6.9	1339	66	84.1	0.7
PC01-1*	681	-21.49	0.07	-114.9	51.0	929	462	88.5	5.1
PC01-2*	682	-20.57	0.02	-63.3	54.1	474	463	93.7	5.4
PC01-3*	683	-21.23	0.01	-165.8	47.9	1404	461	83.4	4.8
PC01-4*	684	-20.85	0.01	-188.1	46.7	1623	462	81.2	4.7
PC01-5*	685	-20.96	0.03	-234.3	44.0	2093	461	76.6	4.4
PC02-1	666	-21.20	0.02	-26.6	16.9	159	138	97.3	1.7
PC02-2	740	-20.78	0.02	-44.9	10.9	317	91	95.5	1.1
PC02-3	667	-20.57	0.03	-197.3	13.9	1716	138	80.3	1.4
PC02-4*	741	-21.10	0.01	-232.2	44.8	2071	469	76.8	4.5
PC03-1	721	-21.67	0.04	-608.3	4.0	7476	81	39.2	0.4
PC03-2	668	-20.89	0.03	-565.8	3.9	6650	71	43.4	0.4
PC03-3	722	-21.40	0.03	-605.3	3.7	7418	76	39.5	0.4
PC03-4	669	-21.41	0.09	-584.9	4.1	7010	78	41.5	0.4
PC05-1*	687	-21.00	0.03	-44.4	55.0	313	462	95.6	5.5
PC05-2	742	-20.89	0.03	-305.9	6.9	2881	80	69.4	0.7
PC05-3	726	-21.42	0.01	-430.4	5.2	4471	72	57.0	0.5
PC05-4	723	-21.57	0.03	-583.8	5.3	6991	101	41.6	0.5
PC06-1*	739	-21.01	0.02	-257.4	42.8	2339	463	74.3	4.3
PC06-2*	691	-21.51	0.02	-411.6	34.2	4209	467	58.8	3.4
PC06-3	672	-21.42	0.01	-400.7	5.6	4061	75	59.9	0.6
PC06-4	673	-20.72	0.02	-333.7	10.2	3210	123	66.6	1.0
PC06-5	674	-21.62	0.03	-438.9	15.9	4599	226	56.1	1.6
PC06-6	676	-22.02	0.05	-524.9	11.9	5928	200	47.5	1.2
PC07-1	671	-21.93	0.03	-552.1	4.2	6401	74	44.8	0.4
PC07-2	728	-21.33	0.01	-536.0	5.0	6117	85	46.4	0.5
PC07-4	738	-21.73	0.06	-637.1	3.5	8091	76	36.3	0.3

* transfer sample, with AMS results corrected to expected normal value

Table IV. AMS results for analysis of TIC from Nankai sediment cores

Sample	NRL ID (AMS)	$\delta^{13}C$ (‰)	$\sigma(\delta^{13}C)$ (‰)	$\Delta^{14}C$ (‰)	$\sigma(\Delta^{14}C)$ (‰)	CRA (ybp)	σ(CRA) (ybp)	pM (%)	σ(pM) (%)
MC01-1	632	-4.38	0.15	-56.6	17.0	417	144	94.3	1.7
MC01-2	633	-3.83	0.15	-165.9	12.3	1406	118	83.4	1.2
MC03-1	654	-4.02	0.15	-156.7	7.1	1317	67	84.3	0.7
MC03-2	655	-3.60	0.15	-195.5	10.5	1696	105	80.4	1.1
PC01-1	596	-2.44	0.15	-110.0	9.5	885	85	89.0	0.9
PC01-2	597	-2.43	0.15	-159.3	12.9	1342	123	84.1	1.3
PC01-3	598	-2.50	0.15	-199.4	10.5	1729	105	80.1	1.1
PC01-4	599	-2.46	0.15	-234.8	10.5	2100	110	76.5	1.1
PC01-5	601	-3.04	0.15	-259.8	8.2	2365	90	74.0	0.8
PC02-1	602	-3.46	0.19	-155.6	11.0	1308	105	84.4	1.1
PC02-2	603	-3.20	0.19	-206.8	11.6	1810	117	79.3	1.2
PC02-3	605	-2.71	0.19	-232.4	7.4	2073	77	76.8	0.7
PC02-4	606	-3.06	0.19	-278.6	8.2	2572	91	72.1	0.8
PC03-1	607	-2.62	0.10	-905.8	6.2	18918	534	9.4	0.6
PC03-2	609	-2.05	0.10	-997.9	1.0	49173	3842	0.2	0.1
PC03-3	610	-3.80	0.10	-997.4	1.5	47857	4760	0.3	0.2
PC03-4	611	-3.26	0.10	-993.6	1.1	40565	1439	0.6	0.1
PC05-1	612	-4.00	0.06	-223.4	8.5	1980	88	77.7	0.9
PC05-2	615	-3.57	0.06	-343.1	7.7	3324	94	65.7	0.8
PC05-3	656	-2.57	0.06	-586.7	5.9	7047	116	41.3	0.6
PC05-3	616	-2.57	0.06	-597.2	5.2	7254	104	40.3	0.5
PC05-4	617	-2.36	0.06	-680.6	4.5	9118	112	31.9	0.4
PC06-1	618	-3.25	0.13	-267.2	9.2	2446	101	73.3	0.9
PC06-2	620	-2.83	0.13	-415.0	6.7	4255	93	58.5	0.7
PC06-3	621	-4.69	0.13	-576.5	7.9	6850	150	42.3	0.8
PC06-4	622	-2.67	0.13	-652.8	4.3	8445	101	34.7	0.4
PC06-5	626	-3.32	0.13	-746.1	7.1	10961	226	25.4	0.7
PC06-6	627	-3.07	0.13	-827.9	7.6	14088	355	17.2	0.8
PC07-1	628	-2.78	0.24	-815.1	6.9	13511	297	18.5	0.7
PC07-2	629	-5.20	0.24	-910.3	3.2	19317	282	9.0	0.3
PC07-4	631	-5.08	0.24	-956.9	2.7	25200	498	4.3	0.3

Table V Maximum apparent sedimentation rate S for each core.

Core	Core Depth (cm)	CRA_{TOP} (ybp)	$\sigma(CRA_{TOP})$ (ybp)	CRA_{BOT} (ybp)	$\sigma(CRA_{BOT})$ (ybp)	S (cm/ka)	$\sigma(S)$ (cm/ka)
MC01	40	1925	151.9	293	68.6	-25	3
MC03	36	737	68.1	1339	66.0	60	9
PC01	197	929*	462.4	2093*	461.2	169	95
PC02	140	159	138.2	2071*	468.5	73	19
PC03	79	7476	80.9	7010	78.3	-170	41
PC05	67	313*	462.5	6991	100.9	10	1
PC06	423.5	2339*	462.7	5928	200.4	118	17
PC07	89	6401	74.4	8091	76.5	53	3

* transfer sample, with AMS results corrected to expected normal value

Table VI Fraction of TIC derived from anaerobic oxidation of methane in each sample

Sample	f_{AOM}	$\sigma(f_{AOM})$
MC01-1	-0.30	0.07
MC01-2	0.06	0.06
MC03-1	0.00	0.06
MC03-2	-0.03	0.06
PC01-1*	-0.08	0.08
PC01-2*	0.03	0.08
PC01-3*	-0.03	0.08
PC01-4*	-0.01	0.08
PC01-5*	-0.04	0.08
PC02-1	0.07	0.06
PC02-2	0.11	0.06
PC02-3	-0.03	0.06
PC02-4*	-0.01	0.08
PC03-1	0.76	0.08
PC03-2	1.01	0.09
PC03-3	1.02	0.09
PC03-4	1.00	0.09
PC05-1*	0.13	0.08
PC05-2	-0.02	0.06
PC05-3	0.22	0.06
PC05-4	0.18	0.06
PC06-1*	-0.06	0.08
PC06-2*	-0.07	0.08
PC06-3	0.24	0.06
PC06-4	0.45	0.07
PC06-5	0.52	0.08
PC06-6	0.62	0.08
PC07-1	0.57	0.07
PC07-2	0.81	0.08
PC07-4	0.89	0.08

* transfer sample, with AMS results corrected to expected normal value

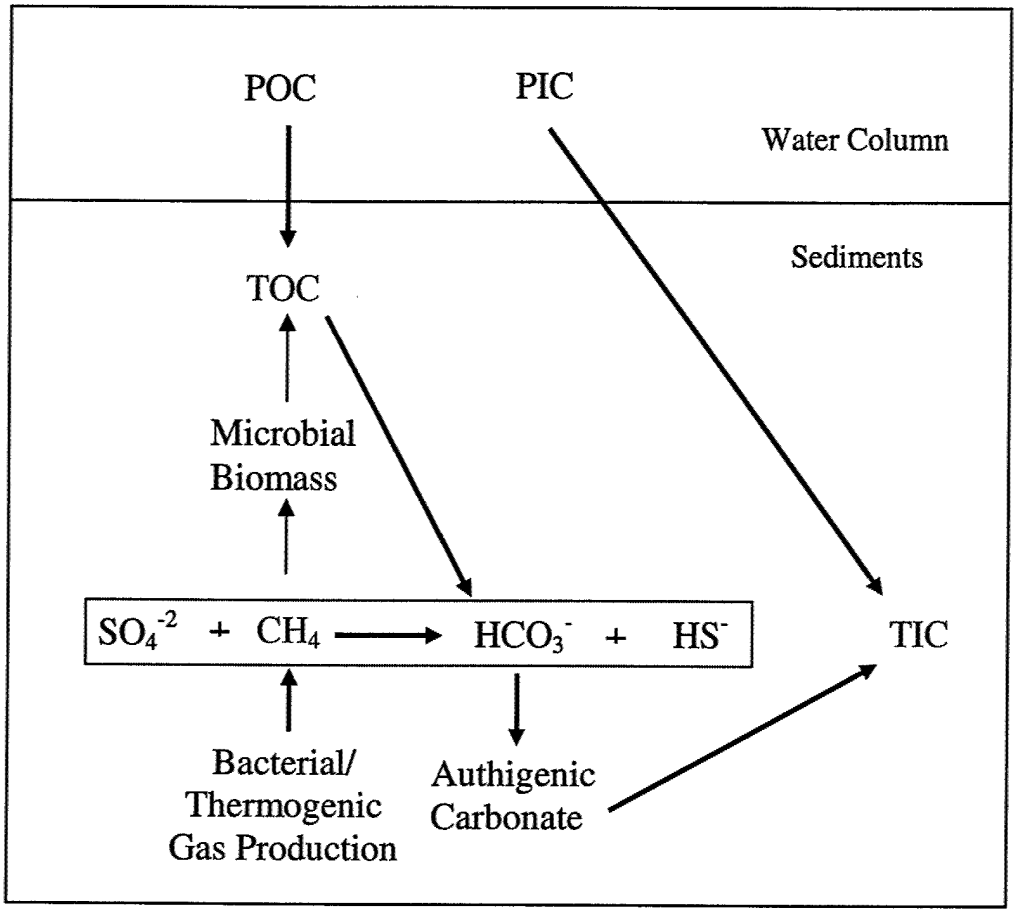

Figure 1. Conceptual model for the biogeochemical cycling of carbon in gas-charged, anoxic, marine sediments. Red text indicates the carbon pools utilized in the isotope based mixing model. POC: Particulate Organic Carbon; PIC: Particulate Inorganic Carbon; TOC: Total Organic Carbon; TIC: Total Inorganic Carbon

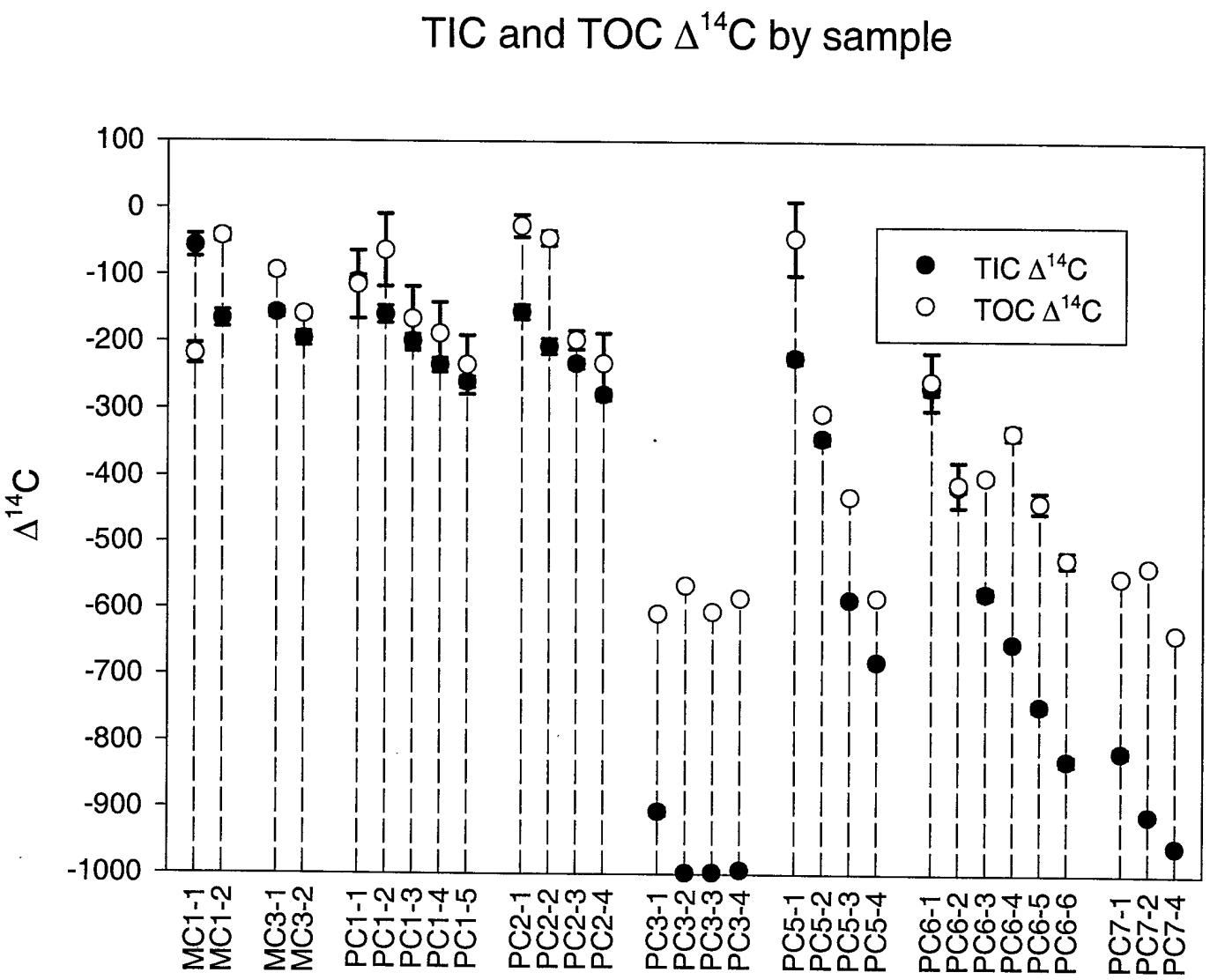

Figure 2. $\Delta^{14}C$ of TIC and TOC carbon pools are shown for each core segment analyzed. Note that the TIC values are generally less that the TOC values. One-sigma error bars are plotted with each data point, but are generally only larger than the symbol size for the nine corrected transfer samples.

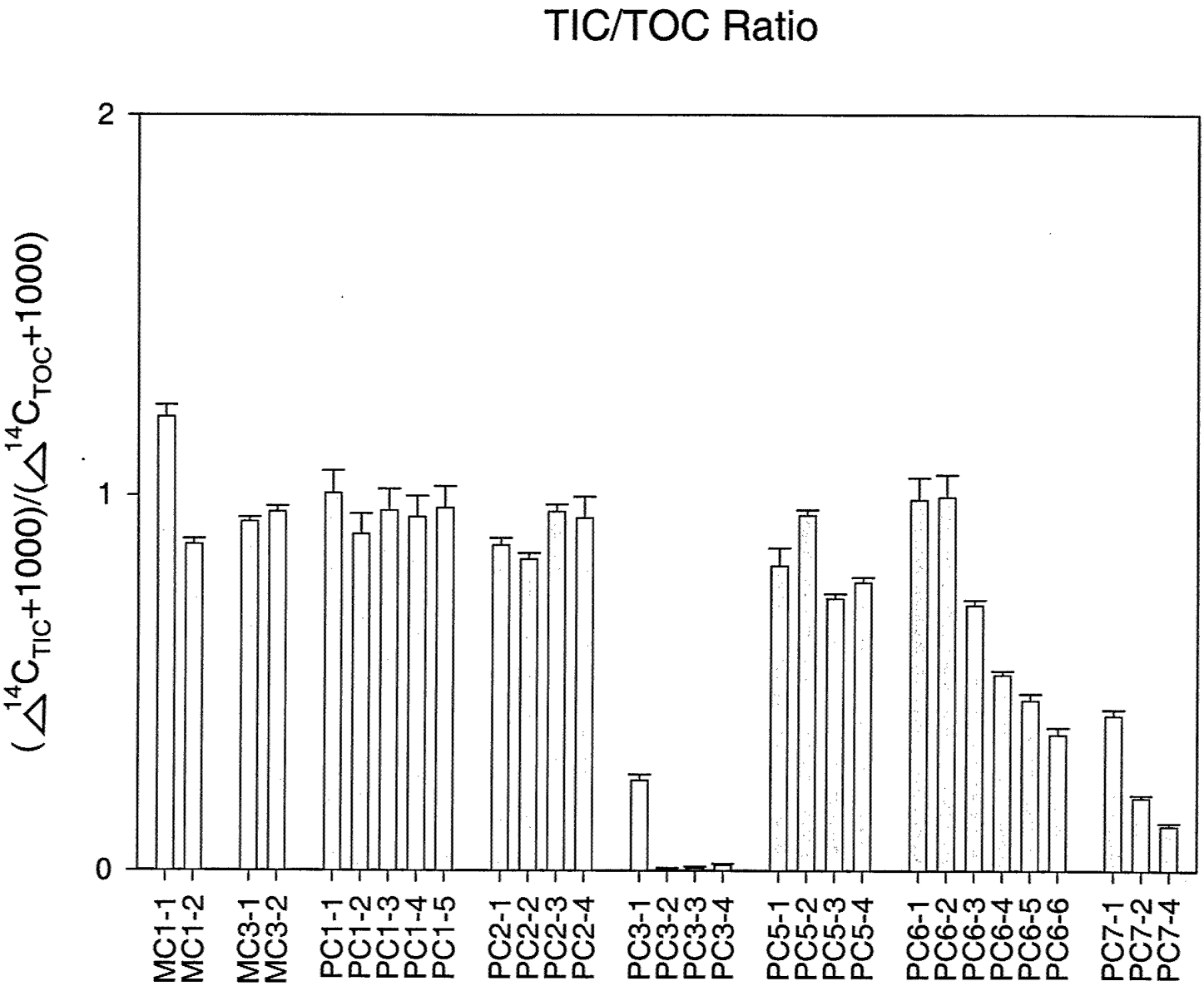

Figure 3. Comparison of relative $\Delta^{14}C$ content in TIC and TOC carbon pools for each core segment analyzed. By taking the ratio shown, the effects of radioactive decay are removed. A ratio below 1 reflects an older age of the source carbon in the TIC compared to the TOC. The offset factor is obtained from the ratio shown for cores PC01 and PC02. One-sigma error bars are shown in the figure.

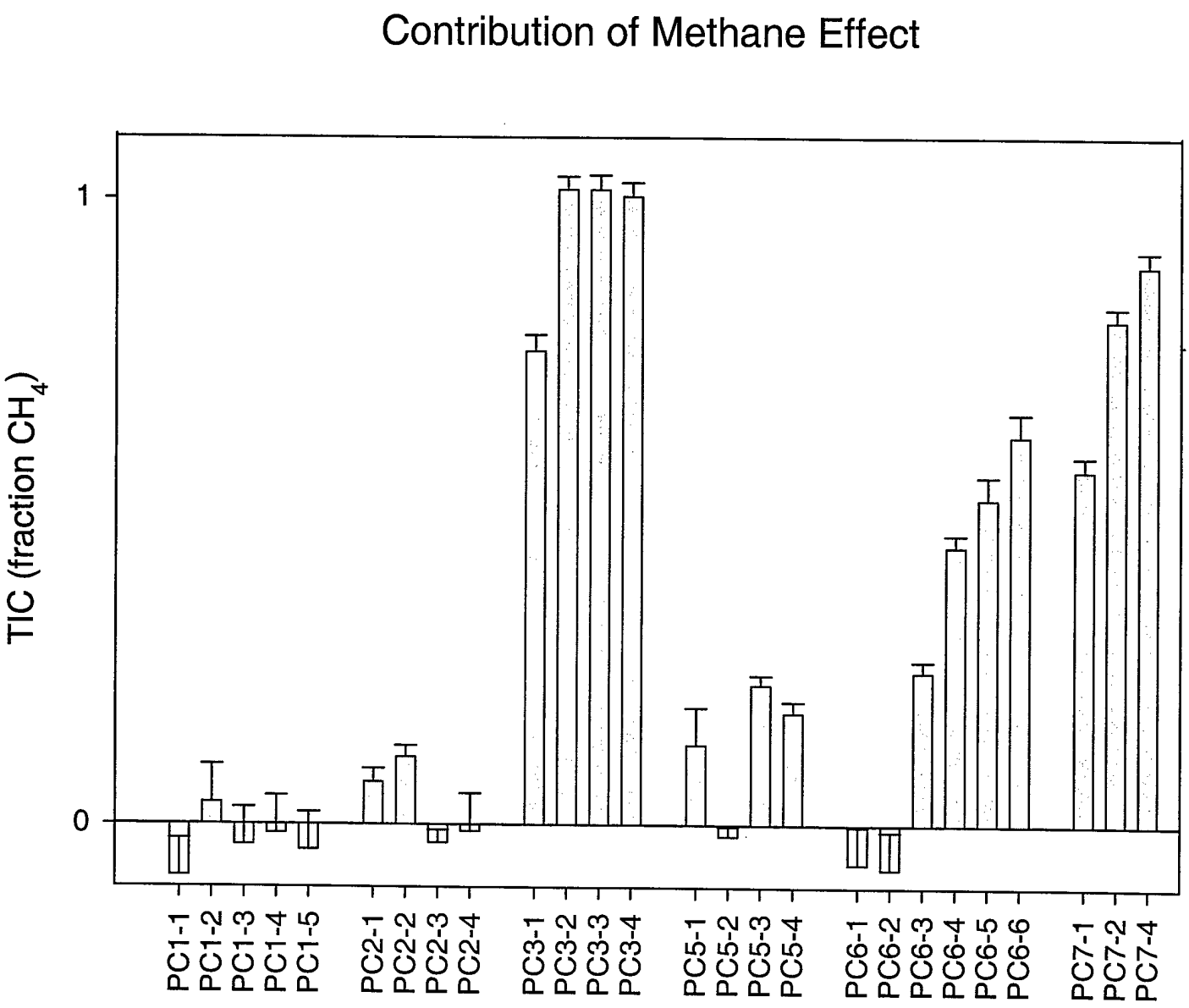

Figure 4. Fraction f_{AOM} of $\Delta^{14}C$ in the TIC carbon pool derived from anaerobic methane oxidation of an ancient methane source, calculated using Eq. 2 for each piston core segment. The largest f_{AOM} is seen in cores PC03, PC06, and PC07. Error bars are one-sigma values.